

Chapter V. Controlled enzymatic degradation of artificial proteins engineered for cell adhesion

Abstract

The ability to tune enzymatic degradation of engineered elastin-like proteins by human leukocyte elastase was investigated. Artificial proteins containing sequences designed to mimic properties of the extracellular matrix for use in medical applications were synthesized. The CS5 domain of fibronectin was included to promote cell adhesion while elastin-like repeats control the mechanical properties. Degradation of polymers containing the VPGIG elastin-like sequence was negligible after 6 h exposure to 0.22 μM elastase ($k_{\text{cat}} = 0.007 \text{ s}^{-1}$, $K_{\text{m}} = 504 \mu\text{M}$), while incorporation of lysine residues within this elastin-like domain, representing a change in 3% of the amino acid side chains, increased the degradation rate such that no intact protein was present after 6 h exposure ($k_{\text{cat}} = 0.033 \text{ s}^{-1}$, $K_{\text{m}} = 2451 \mu\text{M}$). N-terminal sequencing of proteolytic fragments identified the peptide bond directly following isoleucine as the preferred site of cleavage. These engineered proteins were then crosslinked into freestanding, implantable films and subjected to elastase degradation. Incorporation of lysine residues within the elastin-like domain resulted in a 7-fold increase in the film degradation rate compared to the VPGIG elastin-like protein. These results demonstrate the usefulness of protein engineering to create novel, cell-adhesive biomaterials with tunable initial moduli and degradation properties.

Manuscript prepared for submission by Sarah C. Heilshorn, Paul J. Nowatzki, Tetsuji Yamaoka, and David A. Tirrell.

1. Introduction

Engineered proteins are an attractive class of biomedical materials due to their templated biosynthesis, which allows precise control of molecular architecture. Genetic engineering techniques employ microbial cells to synthesize protein polymers with specific sequence, molecular weight, and functionality. This strategy has been utilized in the *de novo* design of artificial proteins exhibiting a variety of novel structural and biomimetic properties.¹⁻⁸ These materials have potential as scaffolds for tissue engineering, drug delivery vehicles, and implantable materials for tissue reconstruction.

Artificial proteins containing elastin-like repeats are of particular interest due to their high expression levels, ease of purification, biocompatibility, and tunable mechanical properties.⁹⁻¹² The extensive work of Urry et al. on the family of elastin-like polypentapeptides (VPGZG)_x, where Z is any amino acid, has shown that the hydrophobicity of the biopolymer can be used to tune the lower critical solution temperature (LCST).^{13,14} At temperatures below the LCST, the polymers are completely soluble, while above the LCST, phase separation into a polymer-rich coacervate occurs. This phase transition behavior allows use of a simple thermal cycling technique to purify crude preparations of elastin-like polymers. Tests of mutagenicity, toxicity, antigenicity, pyrogenicity, and thrombogenicity on elastin-like materials containing GVGVP repeats yielded good results.¹⁵ Lysine residues were genetically engineered into these elastin-like polymers as crosslinking sites to create freestanding protein films.^{9,12} By judicious placement of lysine residues, the molecular weight between crosslinks can be specified, thereby controlling the elastic modulus of the resulting biomaterial within the range of 0.1-1.0 MPa.^{9,12}

To promote cell interactions with these biomaterials, various cell-binding domains have been interspersed with the elastin-like structural units.^{10,11,16} The CS5 domain, located within the alternatively spliced IIICS region of fibronectin, and the RGD domain, located within the tenth type III domain of fibronectin, promote sequence specific spreading and

adhesion of human umbilical vein endothelial cells (HUVEC) when incorporated into elastin-like polymers.^{11,17} These materials exhibit many of the characteristics desirable for use as small-diameter vascular grafts including elasticity similar to natural blood vessels and adhesion of endothelial cells.¹² Based on these positive results, Notch domains have also been engineered into elastin-like proteins as an attempt to control neural stem cell signaling.¹⁸

Regardless of the desired medical application, the use of biomaterials is contingent upon the *in vivo* degradation characteristics of the bulk material. The appropriate degradation rate will be determined by the specific medical application (e.g., drug delivery or tissue regeneration) as well as site of implantation (e.g., cardiovascular system or central nervous system). Therefore, the ability to tune the degradation rate of these biopolymers would be an advantage when designing proteins for specific medical uses. Numerous enzymes with proteolytic capabilities exist *in vivo*; however, native elastin is resistant to many of these proteases with the notable exception of elastase.¹⁹ Therefore, this study seeks to quantify the elastase degradation of engineered elastin-like materials and develop strategies by which this degradation rate can be tuned. In traditional synthetic biomaterials, a variety of strategies have been employed to control degradation rates. These include optimization of polymer chemistry to tune the concentration of hydrolysable bonds,²⁰⁻²² blending of polymers with varying degradation characteristics, and inclusion of peptides into a synthetic polymer network to promote sequence-specific degradation by matrix metalloproteinases.²³ In this work, we employ a genetic engineering approach to design synthetic proteins with tunable elastase degradation rates.

Elastase belongs to the trypsin-like serine protease family of homologous proteins that includes trypsin, chymotrypsin, plasmin, and thrombin. Two forms of elastase are commonly found in humans, pancreatic elastase and leukocyte elastase (HLE, also known as lysosomal elastase, granulocyte elastase, polymorphonuclear elastase, and neutrophil elastase), which differ in substrate specificity and inhibitor sensitivity. Crystallographic

structures and kinetic analyses using synthetic peptide substrates have been used extensively to describe and characterize the catalytic activity of serine proteases.²⁴ The “catalytic triad” of trypsin-like serine proteases (consisting of aspartic acid, histidine, and serine) has been identified as the "charge-transfer relay system" that carries out hydrolysis of the peptide bond.²⁵⁻²⁷

HLE preferentially cleaves the peptide bond directly following a small, hydrophobic amino acid side chain.²⁸ Although synthetic peptide studies have suggested that valine is the optimum cut-site for HLE, other side chains including alanine, methionine, leucine, isoleucine, and threonine have been reported as well as the artificial amino acids norvaline and norleucine.²⁹⁻³¹ Unlike other members of the trypsin-like serine proteases, elastase prefers peptides of four or more amino acids.³² Enzyme-substrate contacts remote from the scissile bond are believed to increase the catalytic rate constant. Crystal structure analysis of HLE with the third domain of the turkey ovomucoid inhibitor reveals direct contact with eight residues of the “primary binding segment” spanning from five amino acids prior to the scissile bond to three amino acids after the scissile bond.³³ These data suggest that appropriate genetic engineering of the elastin-like repeat within engineered proteins may be one strategy to allow tuning of HLE degradation rates. Therefore, HLE degradation rates of engineered proteins containing two distinct elastin-like sequences were compared, Figure 1. Degradation analysis and N-terminal sequencing of proteolytic fragments identified favored cut-sites within the engineered proteins, allowed determination of relevant kinetic parameters, and indicated the time-course of the degradation reaction on both uncrosslinked and crosslinked materials.

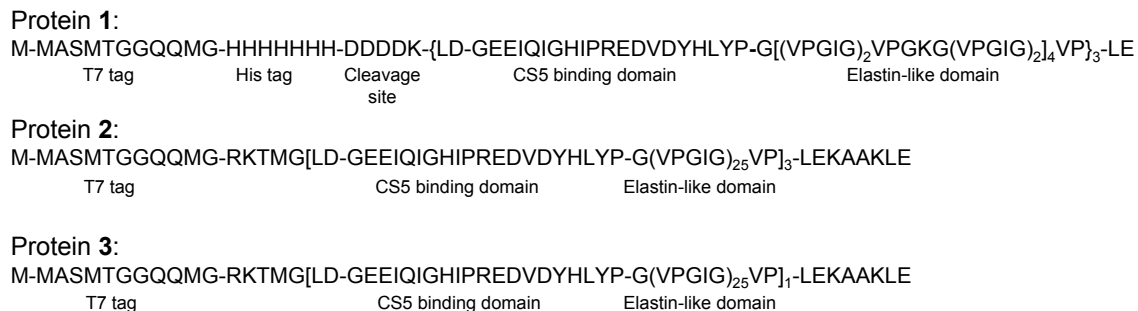


Figure 1. Amino acid sequences of the engineered elastin-like proteins. Protein **1** has three repeats of the CS5 and lysine-containing elastin-like domains. Protein **2** has three repeats of the CS5 and elastin-like domains with lysine residues at the C- and N-termini only. Protein **3** is identical to **2** except it contains only one repeat, decreasing the molecular weight between the lysine residues at the C- and N-termini.

2. Experimental section

2.1. Protein expression and purification

Plasmids encoding sequences **1-3** have been previously described.^{9,12} Proteins were expressed in *E. coli* and purified as previously described.¹¹ Purity was assessed by SDS-PAGE and Western blotting with anti-T7 tag-horseradish peroxidase conjugate antibody (Amersham).

2.2. Analysis of elastase degradation fragments

The degradation reaction was carried out at 37°C for 3 days in sodium borate buffer, pH 8, with 0.22 μ M human leukocyte elastase (HLE, Elastin Products Company, Owensville, MO) and 100 μ M protein **1** or **2**. Samples were taken at 0, 1, 3, 6, 12, 24, 48, and 72 h and diluted with an equal amount of 2X SDS-sample buffer including β -mercaptoethanol and frozen at -20°C. Samples were boiled for 5 min and run on a 12% Tris-tricine gel at 150 V for 1 h. Gels were run in triplicate and either stained with Coomassie blue, transferred to PVDF membrane for N-terminal sequencing of proteolysis fragments, or transferred to nitrocellulose for Western blot analysis using an anti-T7 tag-horseradish peroxidase conjugate antibody (Amersham). Densitometry was performed on

Western blots using Image J (NIH freeware image analysis program) to quantify the amount of whole-length protein remaining at each time point. N-terminal sequencing by Edman degradation was performed on proteolysis fragments at the Caltech Protein/Peptide Micro Analytical Laboratory using a protein micro-sequencer (Applied Biosystems, model 492).

2.3. Kinetics of elastase degradation

The degradation reaction was carried out at 37°C for 6 h in sodium borate buffer, pH 8, with 0.22 μ M HLE and 16-108 μ M protein under constant mixing. The extent of reaction was characterized using 2,4,6-trinitrobenzene sulfonic acid at 4°C to quantify the number of N-termini in solution at 0, 1, 2, 4, and 6 h.

2.4. Crosslinking of protein films

The tri-functional activated ester molecule, tri-succinimidyl aminotriacetate (TSAT), was used to crosslink both **1** and **3**. For each, 30 mg of protein were dissolved in 250 μ L of water at 4°C, and the crosslinker was dissolved in 50 μ L of (25% dimethylformamide / 75% dimethyl sulfoxide) at 4°C; the two solutions were rapidly mixed and pipetted into an open-faced mold. The solvents were removed from the film by drying overnight at 55°C. To achieve similar elastic moduli between the two films, a 0.35:1 ratio of succinimidyl ester functional groups to primary amines was used to crosslink **1**, while a 1:1 ratio was used for **3**.

Matching previous work, **2** was crosslinked with hexamethylene diisocyanate (HMDI) in dimethylsulfoxide³⁴, and **1** was crosslinked with bis(sulfosuccinimidyl) suberate (BS3) in 4°C water.¹² The crosslinker concentrations were chosen such that each film had an initial elastic modulus of ~0.6 MPa, similar to that of native elastin.³⁵ For **1**, the ratio of succinimidyl ester groups in BS3 to primary amines in the protein was 1-to-1; for **2**, a 5-fold stoichiometric excess of isocyanates to primary amines was used.

2.5. Elastase degradation of crosslinked films

Crosslinked films were cut into thin strips of roughly equal protein mass (~3 mg dry); the dimensions (~ 0.25 x 1.5 x 12 mm) were measured after equilibration in PBS, pH 7.4, at 37°C. Samples were exposed to 0.5 mL of elastase solution (final concentration equal to 0.22 μ M in PBS + 0.02% sodium azide as a preservative) at 37°C. At various time points, samples were removed from elastase, equilibrated for 15 minutes to simulated physiological conditions (PBS, pH 7.4, 37°C), and tensile tested with a modified Instron instrument (model 5564). Samples were extended to 20% of their length at a rate of 10% gauge length / min; at this slow rate and minimal extension, viscoelastic effects and hysteresis were observed to be negligible. The elastic moduli were calculated over the initial portion (0-4%) of the stress-strain curves. The samples did not noticeably swell or shrink during the course of the experiment, so the initial cross-sectional area of each sample was used to calculate stress at all time points.

2.6. Weight fraction protein

The protein content of the films was determined from the difference in weight between dry and wet samples. Wet samples were prepared by equilibration in PBS, pH 7.4, 37°C, followed by wicking away of excess buffer with filter paper. The films were then placed at 50°C overnight in a vacuum oven before the dry weights were measured.

3. Results and discussion

3.1. Protein expression and purification

Expression yields for proteins **1-3** were 10, 22, and 7 mg/g wet cell mass, respectively. Aqueous solutions of biopolymers containing elastin-like sequences display a lower critical solution temperature (LCST), above which a polymer-rich coacervate forms and below which the protein is soluble. Therefore, thermal cycling of the wet cell mass provides a facile method of purification of elastin-like proteins. This method was employed

to purify proteins **1-3** in yields of 2.6, 6.6, and 2.1 g, respectively, from 10 L batch fermentations.

3.2. Elastase degradation of engineered proteins with altered elastin-like sequences

The pattern of proteolytic fragments formed by HLE degradation was analyzed by SDS-PAGE, Figure 2. To simulate physiologically relevant conditions, the degradation reaction was performed at 37°C, above the LCST for both proteins. As expected, the variations in amino acid sequence within the elastin-like domains altered HLE degradation of the two synthetic proteins. HLE degradation of protein **1** resulted in many smaller bands of fragments after only 1 h of elastase exposure and complete protein degradation at 12 h. In contrast, degradation of protein **2** resulted in six primary fragments, approximately 3, 12, 15, 27, 30, and 38 kD in mass, and complete protein degradation at 72 h. Therefore, both the time course of degradation and the resulting molecular weights of proteolytic fragments can be altered by replacing the lysine residues within the elastin-like domain of protein **1** with isoleucine residues in protein **2**.

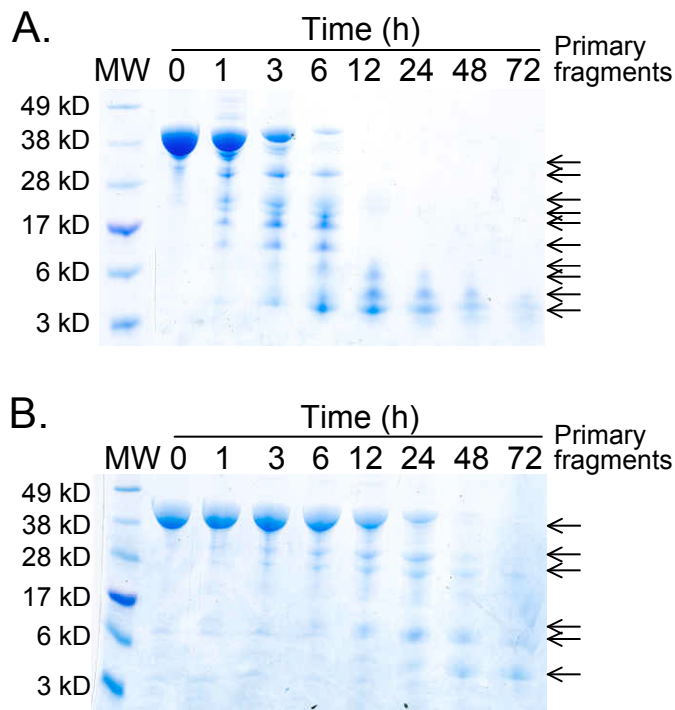


Figure 2. SDS-PAGE of elastase degradation fragments of proteins **1** (A) and **2** (B). Protein **1** is degraded into several fragments that form a “ladder” of molecular weights, denoted by the arrows to the right. Protein **2** degrades into six fragments with approximate molecular weights of 3, 12, 15, 27, 30, and 38 kD, again denoted by the arrows.

N-terminal sequencing of several degradation bands revealed that the peptide bond after isoleucine was the favored cut-site of both proteins **1** and **2**, Table 1. This result was somewhat surprising because previous studies had identified valine as the favored cut-site of HLE, although those studies were performed on small soluble peptides as opposed to the multiple elastin-like repeats contained in these synthetic proteins.^{29,30,36} Protein **1** appeared to cleave preferentially at the isoleucines contained within the elastin-like sequences, resulting in many degradation fragments varying in size by one elastin-unit repeat, while protein **2** preferentially cleaved at the isoleucines contained within the CS5 cell-binding domains. Three of the samples submitted for sequencing also contained fragments with a sequence identical to the N-terminus of the full-length protein. Based on the N-terminal

sequencing results, the cleavage sites and the molecular weight patterns of proteolytic fragments for proteins **1** and **2** were predicted, Figure 3. Consistent with the hypothesis that protein **1** is cleaved at multiple sites within the elastin-like domain, Figure 2A contains a “ladder” of proteolytic fragment sizes. Similarly, the predicted fragment sizes of protein **2** match well with the bands in Figure 2B. From smallest to largest, the fragments in the gel are assigned to the N-terminal sequence alone, one cassette comprising the CS5 and elastin-like domains, one cassette with the N-terminus, two cassettes, two cassettes with the N-terminus, and three cassettes without the N-terminus, which is partially obscured in the gel by the full-length protein.

Table 1. N-terminal sequencing results of selected proteolytic fragments.

Protein	Fragment size (kD)	Called sequence	Protein region of the called sequence	N-terminal cut site of the called sequence
Protein 1	28	GVPGIG	Elastin-like domain	Isoleucine
	28	MMASM	N-terminus	Not applicable
	21	GVPGI	Elastin-like domain	Isoleucine
	17	GVPGIG	Elastin-like domain	Isoleucine
	17	MMASM	N-terminus	Not applicable
Protein 2	15	MMASM	N-terminus	Not applicable
	12	GHIPRE	CS5 domain	Isoleucine

Protein **1**: Full length protein = 37.1 kD

Expected fragment mass sizes = multiple possibilities varying by 1.3, 1.7, and 3.7 kD

M-MASMTGGQMG-HHHHHHHH-DDDDK-{LD-GEEIQIGHIPREDVDYHLYP-G[(VPGIG)₂VPGKG(VPGIG)₂VP]₃-LE

Protein **2**: Full length protein = 43.0 kD

Expected fragment mass sizes = 2.6, 13.4, 16.0, 26.9, 29.5, and 38.1 kD

M-MASMTGGQMG-RKTMG[LD-GEEIQIGHIPREDVDYHLYP-G(VPGIG)₂₅VP]₃-LEKAAKLE

Figure 3. The preferred elastase cleavage sites based on N-terminal sequencing of proteolytic fragments are identified by arrows. Cleavage at these sites would result in the listed fragment mass sizes, which correspond to the proteolytic fragments shown in Figure 2.

It has previously been found that due to the high content of hydrophobic amino acids in the elastin-like domain, various protein fragments stain with Coomassie blue very differently depending on the presence or absence of the T7 tag (unpublished data). Therefore, Western analysis was used to determine the amount of full-length, intact protein remaining after HLE exposure for various times, Figure 4. Densitometry was employed to quantify the percent of full-length protein remaining at each time point, Figure 5. At 6 h, 0% of protein **1** remained intact compared to over 90% of protein **2**. The reaction velocity is constant for both reactions, although protein **2** degrades over a much longer time scale than protein **1**. This suggests that the protein concentration for each reaction is saturating, i.e., the substrate concentration is much higher than the Michaelis constant (K_m), and the reaction rates are at their maximum velocities. (This assumption is validated by more rigorous kinetic testing below, Figure 6.) Therefore, the approximate degradation rate constant, k_{cat} , defined as the maximal reaction velocity divided by the concentration of HLE, is 0.036 s^{-1} for protein **1** and 0.003 s^{-1} for protein **2**.

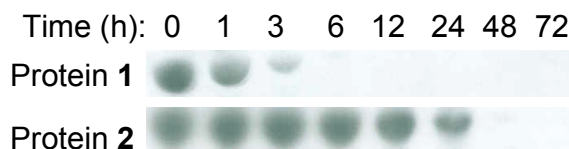


Figure 4. Western blot of full-length, intact proteins **1** and **2** remaining after HLE exposure.

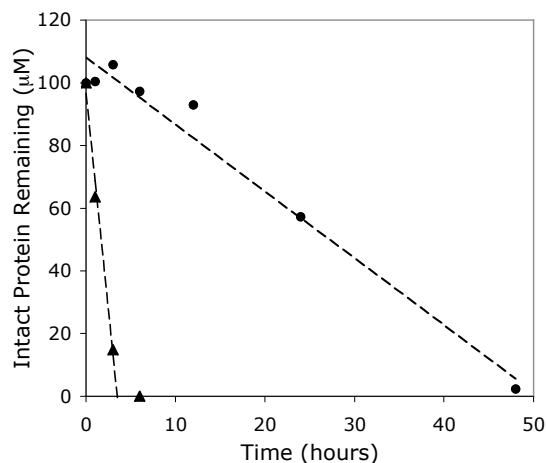


Figure 5. Full-length protein **1** (▲) and **2** (●) remaining after HLE exposure at various time points.

A quantitative analysis was performed using 2,4,6-trinitrobenzene sulfonic acid to determine the kinetic constants of the degradation reaction, Figure 6. Similar to the results above, the initial rate of reaction (the slope of time versus total number of fragments) was found to be linear for both proteins **1** and **2** across all substrate concentrations tested, data not shown. The relationship between initial reaction rate and substrate concentration for both proteins **1** and **2** fit the Michaelis-Menten enzyme kinetic model yielding coefficients of determination, i.e., R values, of 0.95 and 0.77, respectively. Due to the slow degradation of protein **2**, the data had a lower signal to noise ratio and thus more uncertainty was introduced into the parameter fitting. Nevertheless, the determined k_{cat} values of 0.033 s^{-1} and 0.007 s^{-1} for proteins **1** and **2**, respectively, are in good agreement with the degradation rate constants calculated using the simple densitometry method described above.

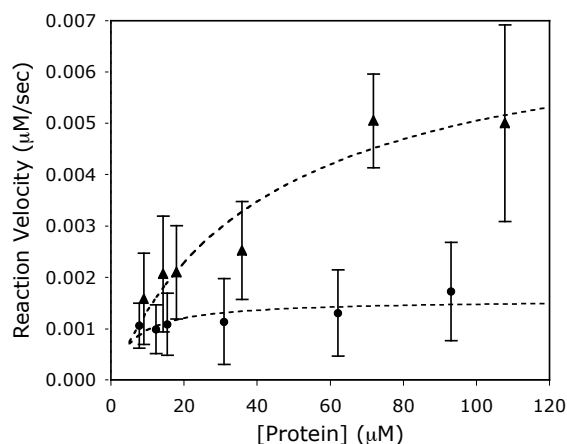


Figure 6. Kinetic analysis of elastase degradation of proteins **1** (▲) and **2** (●). Error bars represent a 90% confidence interval. Dashed lines represent best fits of the observed data to the Michaelis-Menten model.

Because the molecular weight (**1**=37120 Da, **2**=42974 Da) and isoleucine content (**1**=57 residues/chain, **2**=84 residues/chain) of each protein is different, Michaelis constant (K_m) values were determined both as a function of total protein concentration ($K_{m,\text{bulk}}$), which is relevant for bulk material degradation, and isoleucine concentration ($K_{m,\text{Ile}}$), which is relevant for comparison of reaction rates. For protein **1**, $K_{m,\text{bulk}}$ is $43 \mu\text{M}$, and $K_{m,\text{Ile}}$ is 2.45 mM . For the slower degrading protein **2**, $K_{m,\text{bulk}}$ is $6 \mu\text{M}$, and $K_{m,\text{Ile}}$ is 0.50 mM .

Interestingly, $k_{\text{cat}}/K_{\text{m,ile}}$, a measure of the enzyme's "kinetic perfection",³⁷ is similar for both reactions (**1**=13.5 s⁻¹M⁻¹, **2**=13.9 s⁻¹M⁻¹). Therefore, at substrate concentrations much lower than $K_{\text{m,bulk}}$, the two proteins will degrade at similar rates; however, at higher substrate concentrations, which are required for freestanding, implantable films as illustrated below in Figures 7 and 8, the maximal degradation velocities of the two proteins are markedly different.

The time required for the reaction to occur was qualitatively similar to those published in the literature for elastase degradation of elastin and much longer than the times required for the synthetic peptide substrate reactions.^{29,38-40} However, these reports did not analyze the kinetic constants of the degradation of insoluble elastin. Kinetic constants for HLE degradation of plasmin have been reported using an indirect competitive reaction method to measure K_{m} and a direct turbidimetric method to measure k_{cat} . These data report a K_{m} value (0.442 μM) much lower than that of proteins **1** and **2** and a k_{cat} value (0.022 s⁻¹) similar to protein **1**.⁴¹ Meanwhile, the K_{m} and k_{cat} values reported for HLE degradation of soluble synthetic peptide substrates vary from 140-160,000 μM and 0.01-37 s⁻¹, respectively, depending on amino acid sequence.^{29,32}

3.3. Elastase degradation of crosslinked protein films

Freestanding, crosslinked films of the engineered proteins were exposed to HLE, to determine if their degradation rates correlated to those of the soluble proteins. It was desired that the physical properties of the films be as closely matched as possible, to best compare the degradation of the two protein architectures (lysine-rich protein **1** versus proteins **2** and **3** which contain C- and N-termini lysines only). Specifically, the crosslinking chemistries, initial elastic moduli (and thus the molecular weight between crosslinks), water content, and dimensions of the films being compared would ideally be the same. The tri-functional activated ester molecule, TSAT, made meeting these criteria possible; physical properties of the films are listed in Table 2. By substituting the lower-molecular weight protein **3** for the architecturally identical protein **2** in the films, a smaller

molecular weight between crosslinks (M_c), and thus a higher elastic modulus (E) could be achieved. Since protein **1** contains more lysines than protein **3**, a smaller stoichiometric ratio of TSAT was used to make films of similar initial moduli.

Table 2. Physical properties and degradation rates of films of crosslinked elastin-like proteins.

Protein	Crosslinker and stoichiometry	Weight fraction polymer	Sample polymer mass (mg)	E_0 (MPa)	M_c initial (kD/mol)	Degradation rate constant (s^{-1})
1	TSAT 0.35□	0.35	2.8	0.136	25.9	0.0058
3	TSAT 1.0□	0.37	2.6	0.120	31.0	0.0022
1	BS3 1□	0.52	4.0	0.65	8.0	0.0110
2	HMDI 5□	0.73	2.6	0.56	13.1	0.0015

As occurred in the uncrosslinked proteins, films of protein **3** degraded significantly faster than did films of protein **1**, as seen in Figure 7. An approximate first-order rate constant of degradation in each case can be calculated from the linear portion of the degradation curve, if it is assumed that these films behave like ideal networks and that the substrate concentration is saturating. Indeed, the substrate concentration for each film listed in Table 2 is greater than 10 mM, which is about three orders of magnitude larger than the $K_{m,bulk}$ values determined from Figure 6. Similarly, the protein concentration required for a variety of biomedical applications such as tissue engineering scaffolds, drug-delivery vehicles, or implanted materials for tissue reconstruction, would presumably be much larger than $K_{m,bulk}$. Therefore, the degradation reaction will proceed at maximal velocity. HLE is assumed to be able to freely diffuse into the water-rich, highly mobile elastin-like networks; the observed uniformity of degradation throughout the film cross-section supports this assumption. Prior work with these^{9,12,34} and other elastin-like proteins⁴² have shown that the ideal network assumption is a reasonable one. For an ideal rubber network, $E = 3□RT/M_c$ ⁴³; therefore, the molar concentration of effective crosslinks can be defined as the total dry film mass divided by M_c , using a $□$ of 1.3 g/mL⁴⁴. As the film is degraded, the concentration of effective crosslinks is reduced; therefore, the maximal degradation velocity

is defined as the loss in effective crosslinks over time. Analogous to the analysis performed above for the densitometry data in Figure 5, the degradation rate constant is defined as the maximal degradation velocity divided by the molar concentration of HLE; the calculated degradation rate constants are shown in Table 2. Because some peptide cleavages will not result in loss of an effective crosslink, the degradation rate constants calculated from this analysis are smaller than the k_{cat} values determined above; however, they are of the same order of magnitude. Comparing the films made with identical crosslinking chemistry (TSAT), the degradation rate constant of protein **1** is 2.6 times larger than protein **3**.

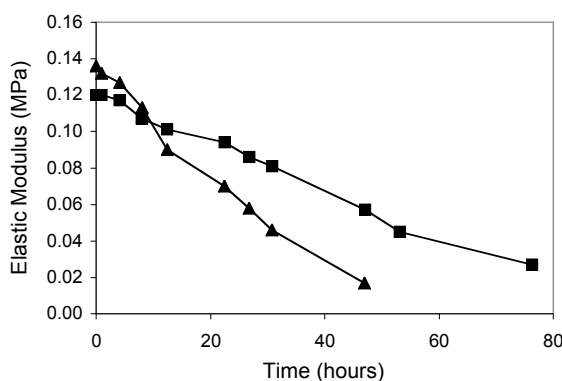


Figure 7. Decrease in elastic modulus after HLE exposure of protein films **1** (▲) and **3** (■) formed with identical crosslinking chemistry.

The difference in degradation rates is also apparent when comparing films prepared with different crosslinking chemistries, Figure 8. Films of protein **1** and protein **2**, crosslinked with bis(sulfosuccinimidyl suberate) (BS3) and hexamethylene diisocyanate (HMDI) respectively, were previously characterized as having initial elastic moduli near 0.6 MPa, typical of native elastin.^{12,34,35} Film **1** exhibited a degradation rate constant 7.3 times larger than film **2**, again mirroring the pattern in the uncrosslinked proteins. The degradation rate constants for these films (Table 2) are similar to those crosslinked with TSAT; differences may result from physical discrepancies, such as in water content, between the films. Taken together, these results demonstrate that crosslinked films of

elastin-like engineered proteins can be designed to have a variety of initial moduli and HLE degradation rates.

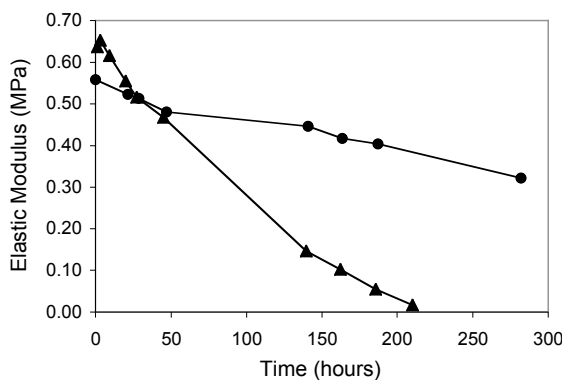


Figure 8. Decrease in elastic modulus after HLE exposure of crosslinked protein films 1 (▲) and 2 (●) formed with differing crosslinking chemistries to yield high initial moduli.

It is important to note that the HLE concentration used in these experiments was chosen somewhat arbitrarily based on previous studies analyzing degradation kinetics of synthetic substrates. The HLE level chosen, 6.3 $\mu\text{g/ml}$ or 0.22 μM , resulted in degradation rates easily quantified over short time scales, i.e., hours and days. This allowed the comparison of various strategies to influence elastase degradation through rational design of the elastin-like sequence. Clinical studies cite HLE levels of 53.3 ± 9.3 ng/ml in human plasma.⁴⁵ HLE activity is tightly regulated *in vivo* by natural inhibitors; therefore, the same concentration of purified HLE will display much higher activity *in vitro*.⁴⁶ Serum levels of HLE are thought to increase in response to sepsis and procedures requiring cardiopulmonary bypass.^{47,48} Decreased inhibition of HLE has also been implicated in the development of pulmonary emphysema and rheumatoid arthritis.^{49,50} For these reasons, future analyses of degradation rates of engineered proteins for specific medical applications will be most instructive if evaluated *in vivo*. This work represents a first step in establishing the kinetics and time-scales of degradation and approaches to tune substrate degradability.

4. Conclusion

This study demonstrates the usefulness of a novel genetic engineering method to synthesize biomaterials with controlled degradation rates for potential medical applications. Two synthetic proteins containing identical cell-binding domains were shown to exhibit altered patterns of HLE degradation based on the amino acid sequence engineered within the elastin-like domain. Through variation in the conditions of crosslinking and genetic engineering of the molecular weight between crosslinks, the moduli of elastin-like synthetic protein films can also be tuned. Control over the initial modulus and degradation rate along with the ability to include cell-recognition domains within the synthetic proteins suggest these materials may be useful in designing tissue engineering scaffolds, drug-delivery vehicles, or implanted materials for tissue reconstruction. Ongoing studies address the *in vivo* degradation and biocompatibility of these and related matrices.

Acknowledgments

This work was supported by NIH Grant 5 ROI HL59987-03 and NSF Grant BES-9901648. N-terminal sequencing was performed by the Caltech Protein/Peptide Microanalytical Laboratory and supported by The Beckman Institute at Caltech.

5. References

- (1) MacPherson, D. T.; Xu, J.; Urry, D. W. *Prot. Express. Purif.* **1996**, *7*, 51-57.
- (2) Petka, W. A.; Harden, J. L.; McGrath, K. P.; Wirtz, D.; Tirrell, D. A. *Science* **1998**, *281*, 389-392.
- (3) Krejchi, M. T.; Atkins, E. D. T.; Waddon, A. J.; Fournier, M. J.; Mason, T. L.; Tirrell, D. A. *Science* **1994**, *265*, 1427-1432.
- (4) Szela, S.; Avtges, P.; Valluzzi, R.; Winkler, S.; Wilson, D.; Kirschner, D.; Kaplan, D. L. *Biomacromolecules* **2000**, *1*, 534-542.

- (5) O'Brien, J. P.; Fahnestock, S. R.; Termonia, Y.; Gardner, K. H. *Adv. Mater.* **1998**, *10*, 1185-1195.
- (6) Kaplan, D. *Nat. Biotechnol.* **2002**, *20*, 239-240.
- (7) Meyer, D.; Chilkoti, A. *Nat. Biotechnol.* **1999**, *17*, 1112-1115.
- (8) Meyer, D.; Chilkoti, A. *Biomacromolecules* **2002**, *3*, 357-367.
- (9) Welsh, E. R.; Tirrell, D. A. *Biomacromolecules* **2000**, *1*, 23-30.
- (10) Panitch, A.; Yamaoka, T.; Fournier, M. J.; Mason, T. L.; Tirrell, D. A. *Macromolecules* **1999**, *32*, 1701-1703.
- (11) Heilshorn, S. C.; Di Zio, K. A.; Welsh, E. R.; Tirrell, D. A. *Biomaterials* **2003**, *24*, 4245-4252.
- (12) Di Zio, K.; Tirrell, D. A. *Macromolecules* **2003**, *36*, 1553-1558.
- (13) Urry, D. W.; Gowda, C.; Parker, T. M.; Luan, C.-H.; Reid, M. C.; Harris, C. M.; Pattanaik, A.; Harris, R. D. *Biopolymers* **1992**, *32*, 1243-1250.
- (14) Urry, D. W.; Luan, C.-H.; Harris, C. M.; Parker, T. M. In *Protein-Based Materials*; McGrath; Kaplan, D., Eds.; Birkahuser: Boston, 1997.
- (15) Urry, D. W.; Parker, T. M.; Reid, M. C.; Gowda, D. C. *J. Bioac. Comp. Poly.* **1991**, *6*, 263-282.
- (16) Nicol, A.; Gowda, D. C.; Urry, D. W. *J. Biomed. Mater. Res.* **1992**, *26*, 393-413.
- (17) Liu, J. C.; Heilshorn, S. C.; Tirrell, D. A. *Biomacromolecules* **2004**, *5*, 497-504.
- (18) Liu, C. Y.; Apuzzo, M. L. J.; Tirrell, D. A. *Neurosurgery* **2003**, *52*, 1154-1165.
- (19) Robert, L.; Robert, A. M.; Jacotot, B. *Atherosclerosis* **1998**, *140*, 281-295.
- (20) Katti, D. S.; Lakshmi, S.; Langer, R.; Laurencin, C. T. *Adv. Drug Deliv. Rev.* **2002**, *54*, 933-961.
- (21) Woo, G. L. Y.; Yang, M. L.; Yin, H. Q.; Jaffer, F.; Mittleman, M. W.; Santerre, J. *P. J. Biomed. Mater. Res.* **2002**, *59*, 35-45.
- (22) Kim, B. S.; Hrkach, J. S.; Langer, R. *Biomaterials* **2000**, *21*, 259-265.

- (23) Lutolf, M. P.; Lauer-Fields, J. L.; Schmoekel, H. G.; Metters, A. T.; Weber, F. E.; Fields, G. B.; Hubbell, J. A. *Proc. Natl. Acad. Sci.* **2003**, *100*, 5413-5418.
- (24) Bode, W.; Meyer, E.; Powers, J. C. *Biochemistry* **1989**, *28*, 1951-1963.
- (25) Carter, P.; Wells, J. A. *Nature* **1988**, *332*, 564-568.
- (26) Craik, C. S.; Roczniak, S.; Largman, C.; Rutter, W. J. *Science* **1987**, *237*, 909-913.
- (27) Creighton, T. E. In *Protein - Structures and Molecular Properties*, 2 ed.; W. H. Freeman & Co.: New York, 1993.
- (28) Geneste, P.; Bender, M. L. *Proc. Natl. Acad. Sci.* **1969**, *64*, 683-&.
- (29) Nakajima, K.; Powers, J. C.; Ashe, B. M.; Zimmerman, M. *J. Biol. Chem.* **1979**, *254*, 4027-4032.
- (30) McBride, J. D.; Freeman, H. N. M.; Leatherbarrow, R. J. *Eur. J. Biochem.* **1999**, *266*, 403-412.
- (31) Harper, J. W.; Cook, R. R.; Roberts, C. J.; McLaughlin, B. J.; Powers, J. C. *Biochemistry* **1984**, *23*, 2995-3002.
- (32) Thompson, R. C.; Blout, E. R. *Biochemistry* **1973**, *12*, 57-65.
- (33) Papamokos, E.; Weber, E.; Bode, W.; Huber, R.; Empie, M. W.; Kato, I.; Laskowski, M. *J. Mol. Biol.* **1982**, *158*, 515-537.
- (34) Nowatzki, P. J.; Tirrell, D. A. *Biomaterials* **2004**, *25*, 1261-1267.
- (35) Abbott, W. M.; Cambria, R. P. In *Biologic and Synthetic Vascular Prostheses*; Stanley, J. C., Ed.; Gurne & Stratton: New York, 1982; pp 189-220.
- (36) Yasutake, A.; Powers, J. C. *Biochemistry* **1981**, *20*, 3675-3679.
- (37) Stryer, L. In *Biochemistry*, 4 ed.; W. H. Freeman & Company: New York, 1995.
- (38) Rao, S. K.; Mathrubutham, M.; Karteron, A.; Sorensen, K.; Cohen, J. R. *Anal. Biochem.* **1997**, *250*, 222-227.
- (39) Reilly, C. F.; Travis, J. *Biochim. Biophys. Acta* **1980**, *621*, 147-157.
- (40) Morrison, H. M.; Welgus, H. G.; Owen, C. A.; Stockley, R. A.; Campbell, E. J. *Biochim. Biophys. Acta* **1999**, *1430*, 179-190.

- (41) Kolev, K.; Komorowicz, E.; Owen, W. G.; Machovich, R. *Thromb. Haemost.* **1996**, *75*, 140-146.
- (42) Aaron, B. B.; Gosline, J. M. *Biopolymers* **1981**, *20*, 1247-1260.
- (43) Aklonis, J. J. In *Introduction to polymer viscoelasticity*; Wiley-Interscience: New York, 1983.
- (44) Gosline, J.; Lillie, M.; Carrington, E.; Guerette, P.; Ortlepp, C. *Philos. Trans. R. Soc. Lond. B* **2002**, *357*, 121-132.
- (45) Oudijk, E. J. D.; Nieuwenhuis, H. K.; Bos, R.; Fijnheer, R. *Thromb. Haemost.* **2000**, *83*, 906-908.
- (46) Hornebeck, W.; Potazman, J. P.; Decremoux, H.; Bellon, G.; Robert, L. *Clin. Phys. Biochem.* **1983**, *1*, 285-292.
- (47) Mojcik, C. F.; Levy, J. H. *Ann. Thorac. Surg.* **2001**, *71*, 745-754.
- (48) Gohra, H.; Mikamo, A.; Okada, H.; Hamano, K. I.; Zempo, N.; Esato, K. *World J. Surg.* **2002**, *26*, 643-647.
- (49) Virca, G. D.; Mallya, R. K.; Pepys, M. B.; Schnebli, H. P. *Adv. Exp. Med. Biol.* **1984**, *167*, 345-353.
- (50) Powers, J. C. *Trends Biochem. Sci.* **1976**, *1*, 211-214.